

MICROSTRUCTURE EVOLUTION DURING ROLLER HEMMING OF AZ31B MAGNESIUM SHEET

Amanda Levinson¹, Raja K Mishra², John Carsley², Roger D Doherty¹, Surya R Kalidindi¹

¹Drexel University; 3141 Chestnut Street; Philadelphia, PA, 19104, USA

²General Motors R&D Center; 30500 Mound Road; Warren, MI, 48092, USA

Keywords: AZ31, Roller Hemming, EBSD, Twinning, Shear Bands

Abstract

The evolution of microstructure and texture during multi-pass roller hemming (flanging, pre-hemming and flat hemming) of commercial grade AZ31B-O sheet has been studied using electron backscatter diffraction. The pre-hemming operations were performed with and without local heating using a laser source. It was observed that samples pre-hemmed at room temperature could not be flat hemmed even after applying heat; whereas flat hemming was possible in the sample pre-hemmed with laser heating. The major difference between these samples was the formation of contraction/double twins on the outer radii of the bend in the sample pre-hemmed at room temperature. It is believed that such twins contributed directly or indirectly to the fracture of this sample upon the third pass by leading to the formation of shear bands and/or by significantly hardening the material and not allowing for further deformation.

Introduction

With a lower density and higher specific strength than both aluminum and steel, magnesium has the potential to help the auto industry realize the goal of vehicle weight reduction [1]. Thus far, cast magnesium alloys have found many automotive applications, but the limited room temperature formability of Mg alloys, owing to their hexagonal close-packed (hcp) structure, has been a major hurdle for implementing applications with wrought materials.

The inability of Mg alloys to accommodate large plastic strains at room temperature can be overcome by processing at elevated temperatures. At temperatures as low as 423K Mg alloys undergo dynamic recrystallization (DRX) [2]. Both continuous and discontinuous DRX mechanisms can be activated in Mg alloys at different temperature and strain rate regimes [3]. Temperature, strain rate, initial texture, and the formation of double twins have been shown to influence DRX [4-6].

If magnesium is to be used in automotive outer body panels, it must withstand numerous processing operations, including hemming. After forming to meet shape and design requirements, the inner and outer panels are joined in a hemming operation. This requires the edges of the outer body panel to be bent around the edge of an inner panel. Conventional hemming procedures are conducted at room temperature, but typical Mg sheet alloys cannot be bent to such extreme deformation at room temperature without fracturing.

Previous research has shown that hemming of Mg sheets is possible at elevated temperature [7]. Both press-and-die (Fig. 1(a)) and roller hemming (Fig. 1(b)) have been performed with Mg sheet. Press hemming is a plane strain bending operation where hem steels bend the flange approximately 90° in a two-step process. Roller hemming is a different process in which a roller is driven around the edge of an outer panel at various angles to gradually bend the flange in multiple passes. Roller hemming, unlike press hemming, is not a plane strain bending action but includes a shear component of strain that distributes strain through a different path [8]. Press hemming of AZ31B sheet has been successfully done at a temperature of ~270°C [7]; while AZ31B sheet roller hemmed in four steps using a laser source to locally heat the sample ahead of the roller (Fig. 1) has been performed at ~170°C [9].

This study presents the microstructural evolution accompanying the successive laser-roller passes used to hem AZ31. Electron backscatter diffraction (EBSD) has been used to examine the microstructural changes in the hemmed zone following successive roller passes with and without laser heating. The effects of heat on the deformation mechanisms during this process are discussed.

Experimental Methods

The samples used in this study were prepared from 1.3 mm thick AZ31B-O sheet as follows: 1) flanged in an oven at 300°C in a wiping motion with a flange steel to an open angle of ~98°; 2) flanged as in (1) then roller-hemmed with a laser-roller speed of 50mm/s in four passes to open angles of 60, 30, 0 degrees and a final pass to flatten the hem; and 3) flanged as in (1) then roller hemmed *without* the laser until the second pass (an open angle of 30°). Samples for the EBSD study were prepared by sectioning the flanged and hemmed samples through the thickness of the bend to examine the microstructure. Heat treatment of some of the hemmed samples was done at 375°C in a salt bath. EBSD data from the polished samples were collected using a Leo 1450 scanning electron microscope fitted with a Hikari high speed EBSD camera and TSL data collection system.

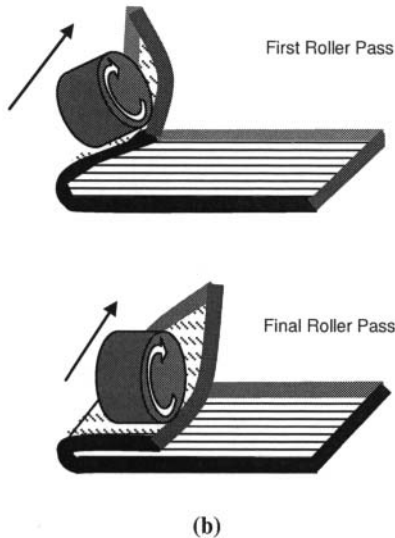
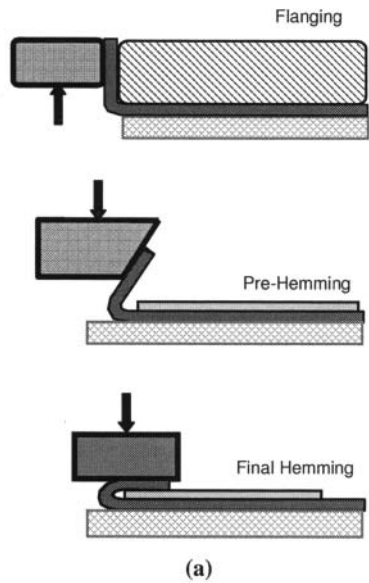


Figure 1. Schematic of, (a) press and (b) roller hemming experimental setup. In laser roller hemming, a laser is placed ahead of the roller.

Results

Flanged Sheet

Figure 2 shows the microstructure of the flanged sample. A banded grain structure was observed at this stage that persisted in each sample after subsequent roller hemming steps. The three bands corresponded to the top tensile zone, bottom compressive zone and the central “neutral” zone of the bent sheet. In regions near the outer (OD) and inner (ID) radii of the bend, nearly defect-free grains, larger than that of the initial material were observed suggesting that these areas have recrystallized. The texture through the thickness of the flanged sheet remains constant, similar to the texture of the sheet before flanging, having a c-axis fiber texture parallel the sheet normal (ND) in all three bands. As will be discussed later, this data suggests

that extension twinning did not play any role in altering the texture in the ID (compression band) at 300°C.

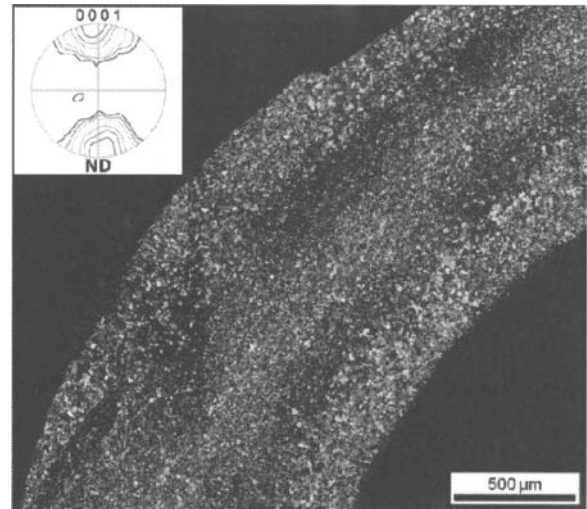
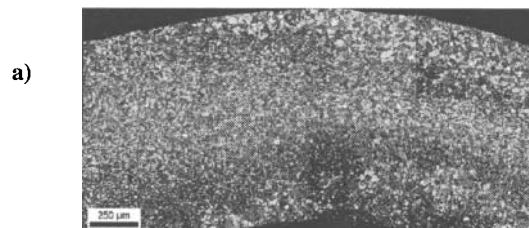


Figure 2. EBSD IPF with respect to the direction normal to the scan after flanging to an open angle of $\sim 98^\circ$. The sheet extends vertically on the left of the image and the flange extends horizontally to the right of the image. The pole figure shows the texture through the thickness of the sheet.

Multi-Pass Laser-Roller Hemmed Sheet

Figure 3 shows the inverse pole figure EBSD maps with respect to the direction normal to the plane of the EBSD scan that illustrate the microstructural evolution during each of the four passes of laser-roller hemming at a roller speed of 50mm/s. The microstructure after each pass exhibited an asymmetrical, banded structure. The grain size along the OD and ID was found to increase until after the second pass. A smaller grain size along the OD and ID developed after the third pass, and it continued to decrease until the fourth and final pass. In this set of samples it was difficult to define an average grain size due to grain size gradients present through the thickness of the sheet as well as around the bend.

The textures for the OD, neutral band and ID along the axis in which the neutral band was the thinnest were measured separately. This location is illustrated on Figure 3(b) and was chosen to maintain consistency of location (and possibly the stress state) in each sample. The OD and neutral bands have a texture similar to the initial microstructure with the basal poles parallel with ND. The ID band has a basal texture component that is rotated $\sim 90^\circ$ from the initial orientation. These texture differences are due to the formation of extension twins in the compressed inner bend that rotated the c-axes by 86° from the ND to the sheet plane, normal to the bend axis.



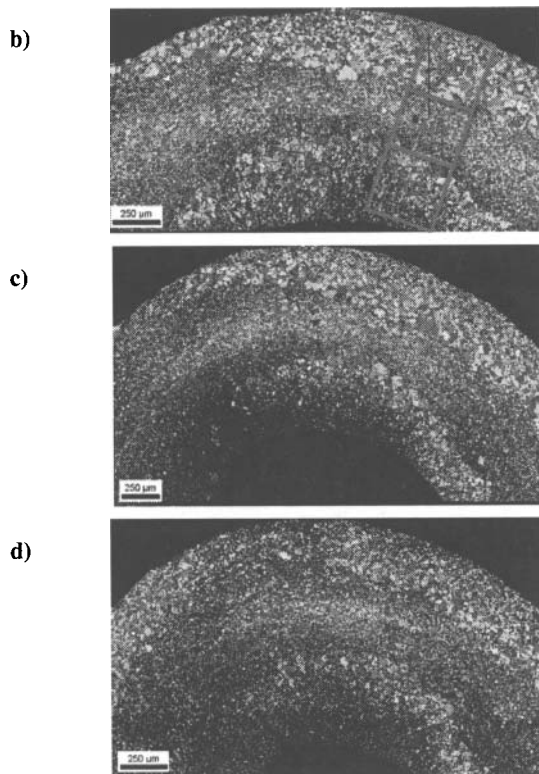


Figure 3. EBSD IPF with respect to the direction normal to the scan of the cross-section after each successive laser-roller hemming pass to open angles of (a) 60°, (b) 30°, (c) 0° and (d) final flat condition. The hem is oriented so the sheet is on the right in all scans. The boxes in (b) show the location of the section chosen to measure texture.

Roller Hemmed Sheet Without Laser Heating

Figure 4(a-b) compares a section of the microstructures of the sample hemmed *without* laser heating to that hemmed with laser heating after pass 2. The sample *without* laser heating was bent through the second pass successfully (to an open angle of 30°); however, further bending of this sample with or without the laser was unsuccessful, resulting in splitting of the hem.

After pass 2, both samples deformed with and without the laser, exhibited a larger grain size along the OD and ID compared to that of the flanged sheet. The textures of the samples hemmed with and without heat were similar to that of the flanged sheet along the OD and neutral axis. Unlike the flanged sample, the textures in the ID band in the rolled samples were rotated by ~90°. The sample hemmed *without* laser heating exhibited a stronger texture component associated with tensile twinning compared to the laser rolled sample.

The major difference between the two samples is the amount and distribution of contraction twinning along the OD. In Figure 4(b), multiple contraction and double twins were observed in the sample hemmed *without* the laser. Bands of low image quality were also present in this sample along the OD and seem to be distributed in a manner suggestive of insipient shear band formation. By comparison, the sample hemmed with a laser exhibited no

contraction or double twinning or any evidence of shear band formation in Figure 4(a).

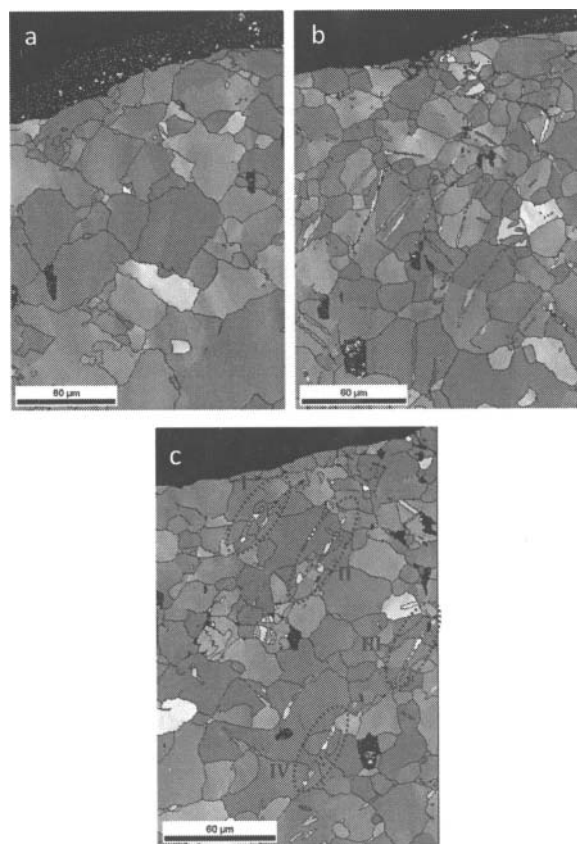


Figure 4. EBSD IPF map with respect to the normal direction of the sheet for the OD of samples hemmed to the second pass with an open angle of 30° under the following conditions; a) with a laser b) *without* a laser, and c) sample (b) followed by a 375°C heat treatment for 1 second in a salt bath. Four areas where recrystallized contraction or double twins have propagated through at least 2 grains in (c) are indicated on areas I-IV.

Discussion

Microstructure and Texture Evolution

High temperature flanging was a critical step during the hemming process as it provided the starting microstructure for the subsequent hemming steps. The banded microstructure that was developed by flanging, with larger grains in the OD and ID regions, was a product of recrystallization. The texture data suggests that during deformation at 300°C, non-basal deformation must have been accommodated by <c+a> type dislocations and very few tensile twins which rotate the c-axis by ~86° must have formed. These few tensile twins are retained in the recrystallized microstructure [10]. Recrystallization and grain growth in the deformed ID and OD bands during and after deformation contribute to a larger grain size whereas no recrystallization and grain growth has occurred in the neutral band which was exposed to 300°C. This banded structure remained throughout the rest of hemming and

likely influenced the extent of different deformation mechanisms and texture evolution, as larger grains have been associated with ease of twinning [11].

At the outer edge of the flange and hem, a tensile strain is present along the OD band causing a contraction along the *c*-axis in most grains. In this orientation, Mg can only accommodate strain by either $\langle c+a \rangle$ pyramidal slip or contraction/double twinning. Contraction twins are thin and hard to detect using EBSD [12] due to their size and increased dislocation density. Although some twins were observed along the OD band, especially in the room temperature roller hemmed samples, either by measuring the misorientation relationships or by poor image quality bands, they did not comprise a large enough volume fraction of the material along the OD to significantly alter the texture. Therefore, the texture along the OD in all samples remained consistent with the starting sheet, having a strong *c*-axis fiber parallel with ND.

The compressive strain in the ID band can be accommodated by stretching the grains in this band normal to the sheet normal (ND). At low temperatures, where $\langle c+a \rangle$ slip is difficult, Mg alloys typically accommodate this strain state through tensile twinning. The texture observations from the ID bands in hemmed samples suggest that the grains in this band deformed by tensile twinning aligning the *c*-axis parallel to the sheet plane. This texture component became more pronounced after subsequent roller passes, indicating a larger volume fraction of twinned material. The stronger texture component in the ID band observed in samples rolled without the laser indicates more of the deformation in the laser heated sample may have been accommodated by tensile twinning than non-basal slip.

Failure in Sample Without Laser Heating

From the results presented above, it is clear that the heat from the laser affects the deformation behavior of AZ31B during hemming. Without the heat applied by the laser, the defect density after hemming to 30° in 2 passes is high enough to inhibit any further deformation from occurring in subsequent hemming passes. The fact that this sample could not be hemmed even after applying a laser in the third pass suggests that the stored defect density in this sample could not be recovered with the addition of laser heating.

One definitive difference in the microstructures is that contraction and double twins were observed more frequently in the large grains of the OD band in the sample hemmed *without* heat. The lack of these twins in the sample hemmed with heat indicates that the additional heat from the laser activated non-basal $\langle c+a \rangle$ slip to a greater extent; thus retarding the activation of contraction/double twinning. The addition of heat also must alter the dislocation mobility and dislocation interactions and affect stored dislocation density, allowing the material to accommodate further deformation in subsequent passes.

Although the exact failure mechanism of the sample hemmed *without* heat is unknown; the contraction/double twins are thought to play a key role in failure initiation. The twins may directly cause crack initiation and/or be responsible for abnormally high strain hardening rates and subsequent failure upon further straining. By reorienting the lattice either 56° or 38° for

contraction and double twinning respectfully, basal slip can be easily activated inside the twins, resulting in the accumulation of a large amount of shear in these twins. In experiments on single crystal magnesium strained in tension parallel to the basal planes, Hartt and Reed-Hill found that

double twins can exhibit strains approaching 1000 % leading directly to fracture along the twin boundaries [13]. It also has been suggested that these twins are precursors to shear bands [10]; which if formed in this material, could promote a larger scale failure mechanism. Figure 5(a) shows the OD of the sample hemmed *without* a laser with all poorly indexed points partitioned out. These poorly indexed bands were oriented at an angle, reminiscent of shear bands, along the OD. By examining some of these bands in more detail it becomes clear in Figure 5(b) that they are composed of contraction or double twins that have created a network through multiple grains. The networking of contraction twins could support their evolution into shear bands that do not anneal-out upon transient laser heating in the third pass and lead to fracture.

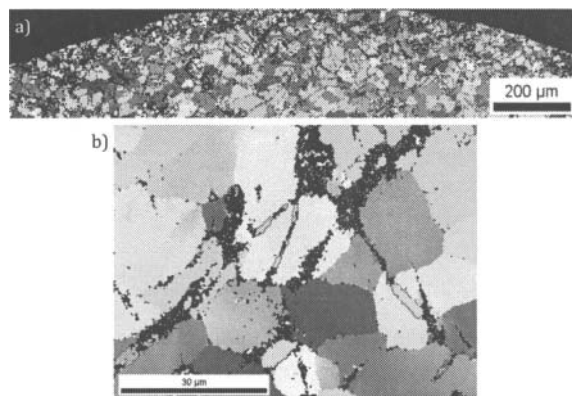


Figure 5. (a) OD of a sheet hemmed to the 2nd pass, an open angle of 30° , *without* the laser. (b) Higher resolution EBSD scan of red box in (a) illustrating that the bands of low quality, which may be shear bands (or precursors to them) are partially composed of double twins that have started to network with twins in neighboring grains.

To explore the potential effect of additional heat on the sample that was hemmed *without* a laser, the sample was heat treated at 375°C (the highest temperature that the surface of the sheet experienced under the laser) for a very short period of time (approximately 1 second) using a salt bath, then quenched in water to approximate the fast heat dissipation between the laser and the roller, the sheet acting as a heat sink. A comparison of the microstructure in the OD region before and after 375°C anneal is shown in figure 4(b-c). It can be seen that some of the contraction/double twins recrystallized from this short heat treatment. Areas in the heat treated sample, Figure 4(c), where recrystallized contraction/double twins extend through at least two grains are indicated by areas I-IV. Recrystallization by bulging did not occur to sweep these small grain zones that would have created a microstructure similar to that in the laser rolled sample after pass 2, leaving areas of very soft material, akin to insipient shear band formation, surrounded

by a hard orientation matrix. Such a microstructure can promote plastic instability leading to shear banding and ultimate failure.

In addition to the differences in the occurrence of contraction/double twins, Fig. 4 shows that many grains retain high intra-grain misorientations. The grains in the laser rolled sample and the annealed sample seem to have retained a high degree of dislocation density. Without quantifying the dislocation density in these samples it is not possible to conclude if the sample rolled without laser has a higher amount of stored work caused by the different deformation modes activated at room temperature, including contraction/double twins that lead to higher work hardening [14] which ultimately led to early failure in pass 3.

References

1. B.L. Mordike, and T. Ebert, "Magnesium: Properties -- applications -- potential," *Materials Science and Engineering A*, 302 (1) (2001), 37-45.
2. A. Galiyev, R. Kaibyshev, and G. Gottstein, "Correlation of plastic deformation and dynamic recrystallization in magnesium alloy ZK60," *Acta Materialia*, 49 (7) (2001), 1199-1207.
3. J.C. Tan and M. J. Tan, "Dynamic Continuous Recrystallization Characteristics in Two Stage Deformation of Mg-3Al-1Zn Alloy Sheet," *Materials Science and Engineering A*, 339 (1-2) (2003), 124-32.
4. Al-Samman, T. and G. Gottstein, "Dynamic recrystallization during high temperature deformation of magnesium," *Materials Science and Engineering: A*, 490 (1-2) (2008), 411-420.
5. J.A. del Valle and O.A. Ruano, "Influence of texture on dynamic recrystallization and deformation mechanisms in rolled or ECAPed AZ31 magnesium alloy," *Materials Science and Engineering: A*, 487 (1-2) (2008) 473-480.
6. S.W. Xu, S. Kamado, N. Matsumoto, T. Honma, Y. Kojima, "Recrystallization mechanism of as-cast AZ91 magnesium alloy during hot compressive deformation," *Materials Science and Engineering: A*, 527 (1-2) (2009), 52-60.
7. J. Carsley and S. Kim, "Warm Hemming of Magnesium Sheet," *Journal of Materials Engineering and Performance*, 16 (3) (2007), 331-338.
8. J.E. Carsley, "Microstructural evolution during bending: Conventional Vs. Roller hemming," *Trends in Materials and Manufacturing Technologies for Transportation Industries*, TMS (2005) 169-174.
9. J.E. Carsley, "Warm Bending Magnesium Sheet for Automotive Closure Panels," MS&T 2009, Pittsburgh, PA, 25-29 October 2009
10. X. Li, P. Yang, L.-N. Wang, L. Meng, and F. Cui, "Orientational Analysis of Static Recrystallization at Compression Twins in a Magnesium Alloy AZ31," *Materials Science and Engineering: A*, 517 (1-2) (2009), 160-69.
11. M. Barnett, Z. Keshavarz, A. Beer, and D. Atwell, "Influence of Grain Size on the Compressive Deformation of Wrought Mg-3Al-1Zn," *Acta Materialia*, 52 (17) (2004), 5093-103.
12. M.R. Barnett, "Twinning and the ductility of magnesium alloys: Part II. "Contraction" twins," *Materials Science and Engineering: A*, 464 (1-2) (2007), 2007, 8-16.
13. W.H. Hartt and R. E. Reed-Hill, "Internal Deformation and Fracture of Second-order {10-11}-{10-12} Twins in Magnesium," *Transactions of the Metallurgical Society of AIME*, 242 (1968), 1127-133.
14. M. Knezevic, A. Levinson, R. Harris, R.K. Mishra, R.D. Doherty, S.R. Kalidindi. "Deformation twinning in AZ31: Influence on strain hardening and texture evolution" *Acta Materialia*, 58 (2010), 6230-6242.